RADIO SCIENCE Journal of Research NBS/USNC–URSI
Vol. 69D, No. 9, September 1965

Ground-Based Passive Probing Using the Microwave Spectrum of Oxygen[1]

E. R. Westwater

Central Radio Propagation Laboratory, National Bureau of Standards, Boulder, Colo.

(Received April 21, 1965)

The determination of the kinetic temperature structure of the troposphere from ground-based measurements of oxygen emission spectra in the microwave region is discussed. Molecular absorption properties of oxygen and water vapor are reviewed. A new "inversion" technique is described. This technique uses a least squares-iteration solution which is applicable to Fredholm integral equations of the first kind. The inversion technique is used to reconstruct two types of tropospheric temperature profiles. The effects of certain types of errors in the brightness temperature on the derived temperature distribution are computed.

1. Introduction

In a recent paper by Meeks and Lilley [1963], the microwave spectrum of oxygen in the atmosphere was discussed. In particular, it was pointed out that measurements of the emission spectrum of oxygen, such as could be taken from a satellite, could be used to determine significant information about the "gross" temperature structure from 40 km down to the earth's surface. In the work reported here, the possibilities of determining the "fine" temperature structure of the lower 10 km by ground-based measurements of the oxygen emission are discussed. The techniques discussed here are applicable only for conditions in which there are no clouds in the main beam of a highly directional antenna.

In sections 2 and 3, the relevant properties of microwave atmospheric radiation and its measurement are reviewed, and calculations of the emission spectrum are presented.

A new method of inverting the radiation measurements to determine the temperature profile is presented in section 4. This inversion technique utilizes a variational iterative method of solving integral equations, and has the advantage over conventional inversion techniques of stabilizing the system against errors both in measurement of the radiation intensity and in estimating the transmission along the ray trajectory.

In section 5, the inversion technique is applied to various atmospheric profiles and the computations of the effects of errors in the brightness temperature on the derived temperature distribution are presented.

2. Background

The amount of radiation flowing in any radiation field is conventionally described by the amount of radiant energy, dE_ν, in a specified frequency interval $(\nu, \nu+d\nu)$ which is transported across an element of area $d\sigma$ and in directions confined to an element of solid angle $d\omega$ during a time dt. The solid angle is centered around the polar angles (θ, ϕ), measured with respect to the normal to the surface. This energy is expressed in terms of the intensity, I_ν, by [Chandrasekhar, 1960]

$$dE_\nu = I_\nu \cos\theta d\sigma d\omega d\nu dt. \tag{1}$$

The variation of the intensity through a medium is related to the absorptive and emissive properties of the medium. Absorption is usually expressed either as an absorption coefficient, α_ν, which is the absorption per unit length, or as a mass absorption coefficient, κ_ν, which is the absorption per unit mass of absorbing material. The two are simply related:

$$\alpha_\nu = \kappa_\nu \rho, \tag{2}$$

where ρ is the mass density of the material.

The emission coefficient, j_ν, is defined as the amount of radiated energy per unit time per unit frequency interval per unit solid angle by an emitter of mass dm. During conditions of local thermodynamic equilibrium, the emission coefficient is related to the Planck function, $B_\nu(T)$, by Kirchhoff's law [Goody, 1964]

$$j_\nu = \kappa_\nu B_\nu(T), \tag{3a}$$

where

$$B_\nu(T) = \frac{2h\nu^3}{c^2} \frac{1}{e^{h\nu/kT}-1}. \tag{3b}$$

In (3b), h is Planck's constant, k is the Boltzmann constant, c is the velocity of light, and T is the absolute temperature.

The assumption of local thermodynamic equilibrium (LTE) requires that the distribution of molecular energy levels be governed by collisions and that the importance of radiative transitions is negligible in

[1] This research is supported by the U.S. Army Electronics Research and Development Laboratory under MIPR R-61-3-SC-07-91.

maintaining this balance. This implies that the mean time between collisions is much less than the mean radiative lifetimes. For the microwave rotational transitions of water vapor and oxygen considered in this paper, the mean time between collisions is of the order 10^{-10} sec, while radiative lifetimes are of order 10^{+7} to 10^{+8} sec. Thus, at microwave frequencies, assumptions of LTE are quite good up to very high altitudes. This is to be contrasted with some of the infrared and visible absorption bands where assumptions of LTE are valid only in the lowest portions of the atmosphere. The reason for this large difference between different frequency regions is the cubic dependence on frequency of the transition probability [Schiff, 1955].

The expression (3b) for the emission function can be simplified for microwave frequencies by using the Rayleigh-Jeans approximation:

$$B_\nu(T) = 2kT\frac{\nu^2}{c^2}. \tag{4}$$

The Rayleigh-Jeans approximation is derived from the Planck function by expanding the exponential term in the denominator of (3b) in a MacLaurin expansion and retaining only the first two terms. The relative error in using (4) is about 0.1 percent at 60 Gc/s and 300 °K.

The amount of radiation emitted by the atmosphere and received by a radiometer can be determined by integrating the transfer equation along a ray path. This equation is [Goody, 1964]

$$\frac{dI_\nu}{ds} = -\alpha_\nu[I_\nu - B_\nu(T)]. \tag{5}$$

Here, ds is an increment of path length. The solution of (5), evaluated at the ground is

$$I_\nu = I_{\nu,0}e^{-\int_0^\infty \alpha_\nu(s')ds'} + \int_0^\infty B_\nu(s)\alpha_\nu(s)e^{-\int_0^s \alpha_\nu(s')ds'}\,ds, \tag{6}$$

where $I_{\nu,0}$ is the unattenuated intensity of discrete sources lying outside the earth's atmosphere. The first term represents contributions to the received energy from external noise sources attenuated by the intervening medium. The second term may be understood physically as follows: an element along the path emits energy towards earth at a rate equal to $B_\nu\alpha_\nu ds$; this emitted energy is in turn attenuated by the intervening medium by an amount

$$\exp\left[-\int_0^s \alpha_\nu(s')ds'\right];$$

the total contribution is then obtained by integrating all contributions along the ray path. It is desirable to explain the functional dependencies of the variables in (6). The absorption coefficient, α_ν, is an explicit (see succeeding section) function of meteorological parameters such as temperature, pressure, and water vapor density. These parameters are, in turn, functions of position along the ray path, thus making the absorption an implicit function of position. It is this dependence only which has been indicated above. Similarly, the Planck function, which is an explicit function of temperature alone, can be written as a function of position. The intensity received at the ground, I_ν, thus depends on the meteorological profile at every point on the ray path. This dependence is described mathematically by stating that the intensity is a functional (as opposed to a function) of the profile. The intensity may be related to a quantity called the brightness temperature, $T_b(\nu)$:

$$I_\nu = 2k\frac{\nu^2}{c^2}T_b(\nu), \tag{7}$$

which compares the received emissions in a single direction to those of a blackbody at temperature T_b.

A nonideal antenna placed in a radiating medium will receive radiation from all directions for any particular antenna orientation, whereas the brightness temperature as defined above refers to the contributions from only a single direction. The effective brightness temperature, $\overline{T_{b\nu}}(\theta', \phi')$, measured by an antenna pointing in the direction (θ', ϕ') may be expressed as [Forward and Rickey, 1960]

$$\overline{T_{b\nu}}(\theta', \phi') = \frac{1}{4\pi}\int G(\theta', \phi'; \theta, \phi)T_{b\nu}(\theta, \phi)d\Omega, \tag{8}$$

where $G(\theta', \phi'; \theta, \phi)$ is the directional gain function in the direction (θ, ϕ) with respect to the antenna axis, $T_{b\nu}(\theta, \phi)$ is the brightness temperature in this direction, and the integration extends over all solid angles, $d\Omega$. For passive probing purposes, a highly directional antenna with low side lobes is necessary so that the measured effective noise temperature closely approximates the brightness temperature of the desired direction. This may be expressed mathematically as

$$\frac{1}{4\pi}\int G(\theta', \phi'; \theta, \phi)T_{b\nu}(\theta, \phi)d\Omega << T_{b\nu}(\theta', \phi'),$$

where the integration extends over all angles except the solid angle of the main beam. Although it has not been indicated explicitly, the antenna gain function is also a function of frequency, thus further complicating an already complicated situation.

The effective noise temperature of an antenna can be measured directly by a Dicke radiometer. The Dicke radiometer accomplishes this by switching a radio frequency signal between the antenna and a reference noise source at a constant rate. If a difference in noise levels exists between the antenna and reference terminals, a "signal" at the switching rate is introduced. By knowing the reference source temperature and through calibration, the magnitude of the difference between the antenna and a reference source temperature is found and the antenna temperature can be calculated.

This minimum detectable signal can be shown [Drake and Ewen, 1958] to be proportional to $1/\sqrt{B\tau}$, where B is the predetection bandwidth of the receiver and τ is its integration time. Thus, for measurements of high sensitivity, it is necessary to have both a large bandwidth and a long integration time. To study the atmosphere by radiation measurements, a narrow bandwidth and a relatively short integration time are desirable. The narrow bandwidth is desirable because assumptions of monochromaticity considerably simplify calcuations of radiation properties; the integration time must be small enough that the gross temperature and pressure profiles do not change during times of measurement. The integration time could be increased for periods of relative calm. A bandwidth of about 20 Mc/s and an integration time of about 10 sec appear suitable for significant measurements. Within a frequency interval of this magnitude, the source function and the absorption profile remain essentially constant and assumptions of monochromaticity are valid.

3. Gaseous Radiation in the Troposphere

In the part of the microwave region considered here (10 to 100 Gc/s) the principal atmospheric gaseous absorbers and, hence, emitters of radiation, are oxygen and uncondensed water vapor. Water vapor absorption is due to a pure rotational transition at 22.2 Gc/s and the nonresonant contribution of other rotational lines starting around 180 Gc/s and extending well into the infrared [Van Vleck, 1947b]. Oxygen absorption is due to a band of rotational transitions starting at about 53 Gc/s and extending to about 66 Gc/s [Zimmerer and Mizushima, 1961]. Figure 1 shows the calculated wet, dry, and total absorption as a function of frequency. The calculations for a standard atmospheric profile were based on the Van Vleck equations given below. It is evident from this figure that oxygen absorption dominates over that of water, except in the immediate region of the water vapor line. This occurs because of the large density ratio of oxygen to water vapor, since the mass absorption coefficients of the two gases are of the same order of magnitude. For frequencies close to the oxygen complex, water vapor absorption is much less than oxygen, except perhaps for extreme climatic profiles.

Water vapor absorption coefficients in the microwave region may be calculated from the formulas of Van Vleck [1947b],

$$\frac{\gamma^{(H_2O)}}{\rho}=0.0318\left(\frac{\nu}{c}\right)^2\left(\frac{293.0}{T}\right)^{5/2}\exp\left(-\frac{644.0}{T}\right)$$

$$\left\{\frac{\left(\frac{\Delta\nu}{c}\right)}{\left(\frac{\nu}{c}-\frac{\nu_0}{c}\right)^2+\left(\frac{\Delta\nu}{c}\right)^2}+\frac{\left(\frac{\Delta\nu}{c}\right)}{\left(\frac{\nu}{c}+\frac{\nu_0}{c}\right)^2+\left(\frac{\Delta\nu}{c}\right)^2}\right\}$$

$$+0.05\left(\frac{\nu}{c}\right)^2\left(\frac{293.0}{T}\right)\frac{\Delta\nu}{c}. \quad (9)$$

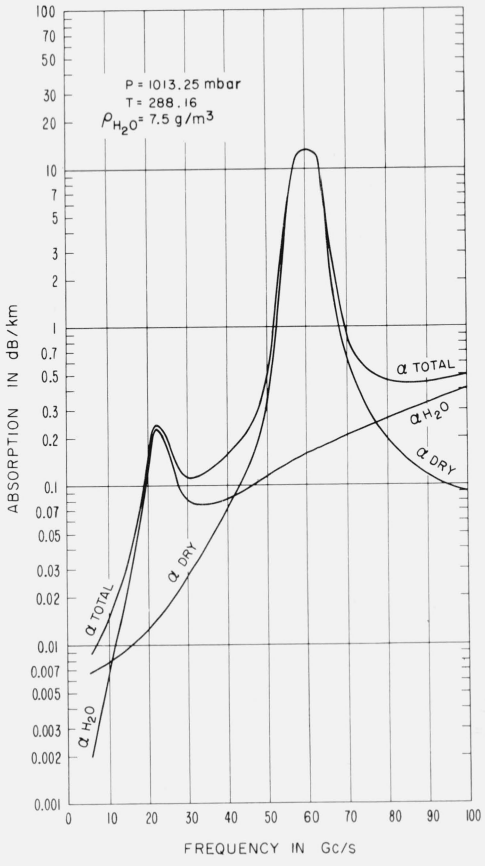

FIGURE 1. *Microwave absorption coefficients at standard surface conditions.*

In (9), $\gamma^{(H_2O)}$ is the absorption (dB/km) at frequency ν (c/s) due to uncondensed water vapor of density ρ (g/m³) at temperature T(°K), ν_0 is the resonant frequency of the water vapor $6_{-5}-5_{-1}$ electric dipole rotational transition (22.235 Gc/s), c is the speed of light, and $\Delta\nu$ is the line width, i.e., the half-width of the line at half intensity. The line width is equal to the reciprocal of the mean time between collisions of the absorbing molecule and depends on the pressure, temperature, and presence of foreign gases. The measured value of the line width at one atmosphere pressure and 318 °K is $\Delta\nu_0=2.6$ Gc/s [Becker and Autler, 1946]. The pressure and temperature dependence of the water vapor line widths have been given as [Barrett and Chung, 1962]

$$\Delta\nu=\Delta\nu_0\left(\frac{P}{1023.25}\right)\left(\frac{318.0}{T}\right)^X(1+0.0046\,\rho). \quad (10)$$

In the above expression, the quantity X as calculated by Benedict and Kaplan [1964] for H_2O-H_2O collisions was found to be 0.614. Calculations by Benedict and Kaplan [1959] for the case of H_2O-N_2 broadening resulted in $X_{N_2}=0.626$ between the temperature ranges of 220 to 300 °K. These calculations indicated a value of $\Delta\nu_0=0.09019$ cm^{-1} (=2.704 Gc/s) at $T=300$ °K.

Recent calculations [Benedict and Kaplan, 1964] have indicated that X_{O_2} is approximately equal to X_{N_2}. These considerations indicate, then, that the temperature and pressure dependence of the water vapor line widths in air may be represented as

$$\Delta\nu_{H_2O} \sim \frac{P_{H_2O}}{P}\left(\frac{T}{T_0}\right)^{-X_{H_2O}} + \frac{\beta_{H_2O-O_2}P_{O_2}}{P}\left(\frac{T}{T_0}\right)^{-X_{O_2}} + \frac{\beta_{H_2O-N_2}P_{N_2}}{P}\left(\frac{T}{T_0}\right)^{-X_{N_2}} \quad (11)$$

where P_m is the partial pressure of the mth molecular species, β_{H_2O-m} represents the relative effectiveness of the mth constituent over H_2O-H_2O collisions in producing water vapor broadening, T_0 is some reference temperature, and $P(=P_{H_2O}+P_{O_2}+P_{N_2})$ is the total pressure of the air. As of yet, there has been no reason to doubt the linear dependence of the H_2O line widths on pressure for the range of pressures normally occurring in the atmosphere.

Oxygen absorption in the microwave region is due to a band of magnetic dipole rotational transitions centered around 60 Gc/s (0.5 cm). The absorption coefficient of oxygen is given by [Van Vleck, 1947a]

$$\alpha^{(O_2)} = \frac{CP}{T^3}\nu^2 \sum_N f_N(\nu) e^{\frac{-E_N}{kT}}, \quad (12)$$

where

$$f_N = \mu_N^2\left[\frac{\Delta\nu_N}{(\nu_N-\nu)^2+\Delta\nu_N^2} + \frac{\Delta\nu_N}{(\nu_N+\nu)^2+\Delta\nu^2}\right].$$

In (12), C is a constant which depends on the units used [Meeks and Lilley, 1963], E_N is the energy of the Nth state, k is the Boltzmann constant, μ_N is the magnetic dipole moment of the Nth state, ν_N is the resonant frequency of the Nth state, N is here a generic label for a particular type of rotational transition, and the other symbols are as defined above.

The oxygen line widths, $\Delta\nu_N$, exhibit a more complicated pressure dependence than do those of water [Abbott, 1964], since the ratio $\Delta\nu/P$ is not a constant with respect to pressure. This behavior is such as to make $\Delta\nu/P$ lower at higher pressures. This has the effect of decreasing the nonresonant absorption while increasing the absorption at a resonant frequency. Measurements have indicated a range of temperature dependence of the line widths from about $X=0.7$ to $X=0.9$ ($\Delta\nu \sim T^{-X}$) [Tinkham and Strandberg, 1955; Artman, 1953], and uncertainties in line width constants of about 10 percent. The ratio of O_2-N_2 broadening to O_2 self broadening has been measured to be 0.75 with an uncertainty of 10 percent.

Figure 2 shows the result of different $\Delta\nu/P$ constants (high- and low-pressure extremes) on the computed noise temperature of the atmosphere. Both curves were calculated using a linear pressure assumption for the line width; the curve corresponding to the actual situation will lie somewhere between these two extremes.[2] These figures indicate that information on line widths could possibly be obtained from radiation measurements of the atmosphere in conjunction with simultaneous meteorological measurements [Abbott, 1964].

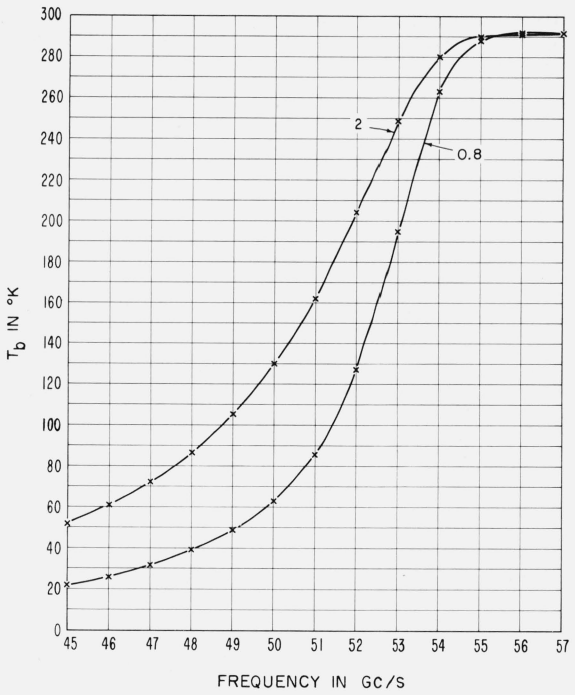

FIGURE 2. *Thermal noise versus frequency for high (0.8 Mc/s/mm* Hg*) and low (2.0 Mc/s/mm* Hg*) pressure values of the line width.*

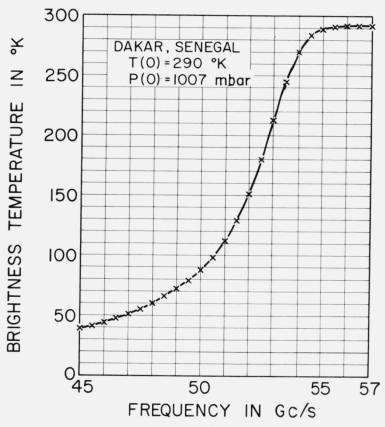

FIGURE 3. *Brightness temperature versus frequency for a vertical antenna.*

A microwave antenna placed in this radiating environment will receive energy at a rate which depends on the frequency, the antenna orientation, and the temperature and density distributions of the atmosphere. For frequencies in the vicinity of the oxygen complex, and for low antenna elevation angles, the

[2] All succeeding calculations reported here will be based on the low-pressure measurements of Artman [1953].

total integrated absorption (optical depth) is so large that the atmosphere is essentially a blackbody radiating at a temperature nearly equal to that at the surface of the earth. For frequencies near the center of the oxygen band, the atmosphere is again a blackbody radiating at nearly the surface temperature for all elevation angles. In the frequency region from 50 to 55 Gc/s and for a vertical antenna, however, a large change in brightness temperature with frequency occurs, as seen in figure 3. Over this relatively small frequency interval, a brightness temperature change of about 150 °K takes place and in the steepest portion of the curve, the slope is about 60 °K per Gc/s. The calculations in this figure were based on radiosonde data from Dakar, Senegal, February 2, 1956. It is to be noticed in this figure that the brightness temperature is greater than the surface temperature for frequencies greater than about 55 Gc/s. This occurs because of a temperature inversion which reached a maximum of about 294 °K at 1 km. In general, the brightness temperature can never be greater than the maximum temperature of the atmosphere.

The possibility is immediately suggested that this portion of the spectrum might be useful for a ground-based passive probe of the lower atmosphere. On a cloudless day, the emission in this region is essentially a function of the temperature alone because of the relatively small water vapor contribution and, hence, measurements of this emission might be used to infer something about the temperature structure of the atmosphere. The large changes in brightness temperature, T_b, over this frequency interval satisfy one of the necessary requirements for a ground-based remote probing system; i.e., that the changes in T_b with frequency are sufficiently large that a nondegenerate set of equations may be obtained for inverting the brightness temperature versus frequency curve to determine the temperature-height profile of the lower atmosphere. The equipment requirements necessary to make relevant measurements have been discussed in section 2.

Another important effect takes place in this frequency region. If the height above which the brightness temperature contribution may be neglected [3] is plotted against the surface absorption coefficient, as is done in figure 4, the layers of the atmosphere which contribute most strongly to the brightness temperature at a given frequency can be determined. In this figure it is evident that the relative contribution from various altitudes is strongly frequency dependent between 52.5 and 55 Gc/s. For frequencies below about 52 Gc/s, the radiation contribution is averaged over a fairly large height interval (~ 17 km); above 55 Gc/s through the center of the oxygen band, the contributions to the brightness temperature are from a narrow height interval close to the ground.

The large slope of the brightness temperature versus frequency curve and the pronounced changes of the

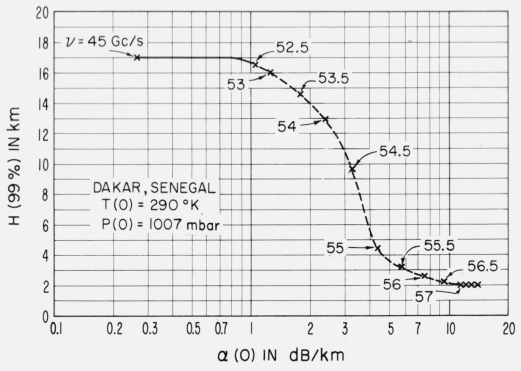

FIGURE 4. *Height above which thermal noise may be neglected (99 percent level) versus surface absorption coefficient.*

radiation cutoff height, as pointed out above, arise because of the large variations in both the absorption coefficient and the optical depth. Thus, in the relatively small frequency interval, both the low and high attenuation limits of the radiation transfer equation occur.

It should be pointed out that both the radiation cutoff height and, as has been seen, the brightness temperature, depend on the manner in which the line width parameters vary with temperature and pressure. Although a more realistic description of this behavior will change the numerical values of the quantities involved, the basic conclusions of this section will remain the same.

4. Basic Equations of the Inversion Process

The brightness temperature, $T_b(\nu)$, at a microwave frequency ν, observed looking up into the atmosphere, is given by [Fryberger and Uretz, 1961]

$$T_b(\nu)=\int_0^\infty T(h)\alpha_\nu(h,\, T(h))e^{-\int_0^h \alpha_\nu(h',\, T(h'))dh'}\,dh, \qquad (13)$$

where T is the absolute temperature (kinetic), α_ν is the gaseous absorption per unit length, and h is the height.[4] The problem to be solved is the determination of $T(h)$ from a set of measurements of $T_b(\nu)$. This solution is referred to as the inversion process. The absorption coefficient α_ν is due to water vapor and oxygen. As is seen in figure 1, in the frequency region 50 to 55 Gc/s, the principal portion of the absorption is due to oxygen, and we will hence neglect the water vapor contribution in the temperature inversion process. It is realized, however, that this assumption is probably not valid for very humid conditions, and future work should take this into account.[5]

Before deriving the inversion equations, a brief review of the relevant concepts and terminology of integral equations will be necessary. A Fredholm

[3] This level has here been chosen as the 99-percent level. A more meaningful choice could be made if the exact experimental capabilities of the radiometer in use were known. For example, if the uncertainty in measurement of T_b were 0.5 °K, then the height level corresponding to this value would be chosen.

[4] Previously, h denoted Planck's constant. In all succeeding parts of this work, h will refer to height.

[5] It is plausible that in conjunction with the oxygen emission measurements, a determination of the tropospheric water vapor distribution could be obtained from radiation measurements taken around the 22.2 Gc/s water vapor line.

integral equation of the first kind is given by [Tricomi, 1957]

$$\phi(x)=\int_a^b \mathcal{K}(x, y)\Psi(y)dy, \tag{14}$$

where $\phi(x)$ and $\mathcal{K}(x, y)$ are known and $\Psi(y)$ is the unknown function. The function $\mathcal{K}(x, y)$ is called the kernel of the integral equation. Equations of the type (14) are linear, i.e., if Ψ_1 is the solution corresponding to ϕ_1, and Ψ_2 is the solution corresponding to ϕ_2, then $a\Psi_1+b\Psi_2$ (a, b are any constants) is the solution of $a\phi_1+b\phi_2$. There are well-known methods for solving or getting approximate solutions of this type of linear equation if the analytic (exact) form of ϕ and $\mathcal{K}$ are known [Morse and Feshback, 1953]. Methods of solution of nonlinear integral equations are, however, not so well known.

In many cases of physical application, ϕ is represented by a set of measured values, and no analytic form is known for the function. These measured values will never be exact because of errors inherent in any physical measurement. Such errors in ϕ give rise to difficulty in the numerical solution of (14) because it is unstable, i.e., a small (infinitesimal) change in ϕ can give rise to a large (finite) change in the sotion Ψ. This can be shown by the following elegant argument given by Phillips [1962]. Consider the well-known theorem true for any integrable function $\mathcal{K}(x, y)$

$$\lim_{k\to\infty}\int_a^b \mathcal{K}(x, y)\sin kydy=0 \tag{15a}$$

or

$$\epsilon(x)=\int_a^b \mathcal{K}(x, y)\sin kydy \tag{15b}$$

where $\epsilon(x)\to 0$ as $k\to\infty$. Equation (15) is sometimes called Dirichlet's integral theorem. If (15b) is added to (14), there results

$$\phi(x)+\epsilon(x)=\int_a^b \mathcal{K}(x, y)[\Psi(y)+\sin ky]dy. \tag{16}$$

If we now interpret ϵ as an error in the measured value of ϕ, it is seen that a small error can add a finite highly oscillatory component to the correct solution Ψ. Such an oscillatory behavior could destroy all physical meaning of the solution.

To determine the vertical temperature distribution from a set of radiation measurements requires a numerical solution of the integral equation (13). This is difficult because (a) the integral equation is nonlinear, i.e., the kernel is a function of the unknown quantity $T(h)$, and (b) this equation is also unstable against errors in the measured quantity $T_b(\nu)$. The difficulty of nonlinearity can be overcome by first linearizing the equation by using a standard model to estimate the kernel, solving the resulting linearized equation, and then iterating, correcting the kernel at each step [Fow, 1964]. The convergence of this iteration sequence depends, *inter alia*, on how the difficulties in (b) can be eliminated. It was found that (before suitable smoothing) reduction of the integral equation to a set of simultaneous equations (to be solved by matrix inversion) can lead to unreasonable estimates of the temperature profile if there are errors present in T_b. By use of the following least-squares method, stability against errors, both in T_b and in estimation of the kernel, was achieved.

To solve (13) for $T(h)$, a standard exponential model, $\alpha_\nu^{(0)}$, is first assumed for the absorption decay with height. This linearizes the equation in this first-order approximation. Next, the infinite upper limit of the integral is replaced by the radiation cutoff height, $H(\nu)$. This height can be very accurately estimated from a standard model. The spectrum of these heights over the chosen frequency range determines an upper limit to the height intervals which can be probed by this method. Equation (13) is now approximated by

$$T_b(\nu)=\int_0^{H(\nu)} T(h)\,\mathcal{K}(\nu, h)dh, \tag{17}$$

where the kernel, $\mathcal{K}(\nu, h)$, is determined by the absorption model, and is a function of height and frequency alone.

The temperature, $T(h)$, can now be determined by inverting (17). A polynomial expansion is chosen for $T(h)$,

$$T(h)=\sum_{i=0}^{N} t_iU_i(h), \tag{18}$$

where the set of $\{t_i\}$ is to be determined and $U_i(h)$ is some polynomial of degree i. Substituting (18) into (17),

$$T_b(\nu)=\sum_{i=0}^{N} t_iK(\nu, i), \tag{19}$$

where

$$K(\nu, i)=\int_0^{H(\nu)} U_i(h)\alpha_\nu^{(0)}(h)e^{-\int_0^h \alpha_\nu^{(0)}(h')dh'}dh.$$

Rather than solve (19) in its unstable form by matrix inversion, consider the quantity I, defined as

$$I=\sum_{j=1}^{N_\nu}\left[T_b(\nu_j)-\sum_{i=0}^{N} t_iK(\nu_j, i)\right]^2 + 2\sum_{k=N+1}^{N+N_B}\gamma_k\left(\sum_{i=0}^{N} t_iU_i(h_k)-T(h_k)\right), \tag{20}$$

where the j-summation ranges over frequencies, the k-summation ranges over the known boundary condi-

tions on the temperature at the height h_k, and γ_k are undetermined Lagrange multipliers. The quantity I, except for the constraint terms in the summation over k, may be understood as follows. Each term of the frequency summation (over j) can be recognized as the square of the difference of the "measured" brightness temperature, $T_b(\nu_j)$ and the computed brightness temperature at that frequency. The computed brightness temperatures are determined completely when the set $\{t_i\}$ is given. It is reasonable to assume that the set of these coefficients which *minimizes* I is the best approximation to the temperature profile for the given set of radiation measurements and choice of polynomial degree. Thus, it is required that the variation of I with respect to the parameters, $\{t_i\}$, be a minimum. Setting the appropriate partial derivatives of I with respect to t_k equal to zero yields, for N_ν frequencies, N_b boundary conditions and an Nth degree polynomial,

$$\sum_{i=0}^{N} t_i A_{ik} + \sum_{j=N+1}^{N+N_b} \gamma_j U_k(h_j) = D_k, \qquad k = 0, 1, \ldots, N \tag{21}$$

where

$$A_{ki} = A_{ik} = \sum_{j=1}^{N_\nu} K(\nu_j, i) K(\nu_j, k)$$

and

$$D_k = \sum_{j=1}^{N_\nu} T_b(\nu_j) K(\nu_j, k).$$

Equations (21), together with the N_b constraining equations on the temperature, suffice to determine the set $\{t_i\}$. Equations (21) would be modified if the derivatives of the $\mathscr{K}$ functions were included. These derivatives are small, since the kernel is not a sensitive function of temperature, and hence are neglected.

An iteration process can now be set up in the following manner. From the temperature distribution derived above and the relation [Hewson and Longley, 1944],

$$\left(\frac{P_2}{P_1}\right) = \left(\frac{T_2}{T_1}\right)^{\frac{Mg}{Rl_{12}}}, \tag{22}$$

which determines the pressure between any two layers in the atmosphere which have a constant lapse rate, a new set of absorption coefficients and kernel functions can be obtained from (12) as a function of height in the atmosphere. In (22), M is the molecular weight of air, g is the acceleration of gravity, R is the general gas constant, and l_{12} is the lapse rate between layers 1 and 2. A numerical integration is then performed using the derived set of absorption coefficients to determine a new set of functions $K(\nu, i)$ of (19), taking fully into account the temperature and pressure dependence of the absorption coefficients and the line widths. Equations (21) are again used to determine the $\{t_i\}$ by utilizing the new estimate of the kernels. The iteration process is then continued until a self-consistent set of temperature coefficients is obtained. By self-consistency, it is here meant that neither the kernel functions nor the set $\{t_i\}$ changes from the Nth to the $(N+1)$th iteration.

The numerical integration of the kernel functions of (19), for a polynomial of arbitrary degree and with exponential absorption within any level, is nontrivial. The details of this integration are shown in appendix A.

It should be mentioned that the least-squares method presented above is quite general and could be used for other types of assumptions for the temperature distribution such as exponential, trigonometric, constant layer, etc. The number of parameters that can be determined accurately is, of course, basically limited by the inherent instability of the integral equation.

5. Application of Inversion Method

In this section, the inversion technique described in section 4 is applied to atmospheric temperature and pressure profiles from Denver, Colo., and Dakar, Senegal. The brightness temperatures were calculated using the radiosonde data from the two stations; from this basic set of numbers, the inversion method of section 4 was applied in an attempt to reconstruct the original profile. The Denver profile was chosen because of close similarity to a standard profile; Dakar illustrates the effects of a strong temperature inversion at low altitudes.

In figures 5 and 6, the inversion of the August 16, 1953, Denver, Colo., profile is shown. The inversion was accomplished by using 12 frequencies to fit a fourth-degree polynomial which was constrained below by the surface temperature and above (at 16.0 km) by a standard atmosphere temperature. The derived profile of the lower atmosphere is insensitive

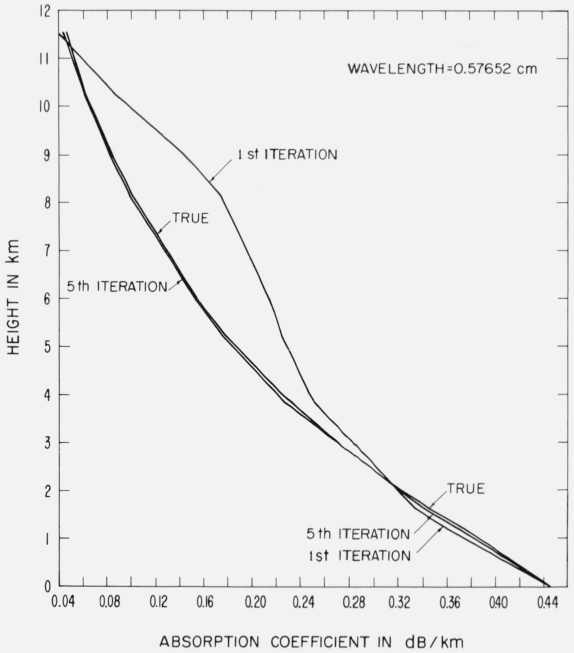

FIGURE 5. *Absorption profile as determined by inversion of the brightness temperature equation for profile of Denver, Colo.*

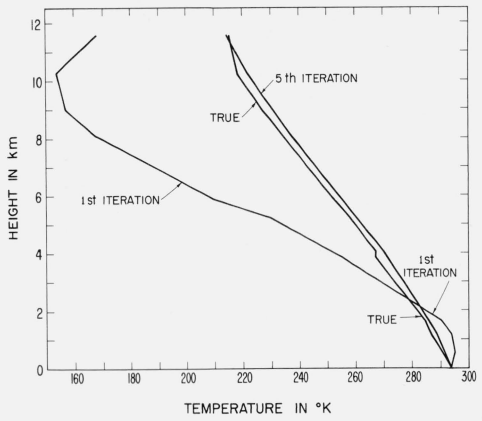

FIGURE 6. *Temperature profile as determined by inversion of brightness temperature equation for a Denver, Colo., profile.*

to the choice of this upper constraint. The iteration sequence converged to the indicated values on the fifth iteration. It is to be noted that convergence occurred even though the first approximation, as determined by a crude absorption model, is very far from the correct values. It is also to be noted that, after a sufficient number of iterations, the computed absorption profile is almost coincident with the actual, even though there is a residual error in the temperature prediction. This is due to the relative insensitivity of the absorption coefficient to small temperature changes.

The errors in the computed temperature structure up to the Nth height level may be expressed in terms of the rms error in T, S.E. (T), defined by

$$\text{S.E.}(T)=\sqrt{\frac{1}{N}\sum_{i=1}^{N}(T(h_i)-T^c(h_i))^2}, \qquad (23)$$

where $T(h_i)$ and $T^c(h_i)$ are the actual and computed temperatures, respectively, at the ith height level, h_i. For the profile just discussed, the rms error in T up to 11.6 km was 41.8 °K for the first iteration, and was reduced to 2.6 °K after five iterations. The corresponding errors for the pressure were 27.6 and 1.6 mbar, respectively. Table 1 gives the calculations of the rms errors in T and P up to the 11.6-km level at each step in the iteration process.

TABLE 1. *The rms error in temperature and pressure up to 11.6 km as a function of iteration number for Denver, Colo., August 16, 1953*

Iteration	rms error in T	rms error in P
	°K	*mbar*
1	41.8	27.6
2	34.1	21.0
3	23.1	13.4
4	10.2	5.3
5	2.5	1.6

The method of this paper is also capable of determining temperature inversions, as may be seen in figure 7. The Dakar, Senegal, profile of February 2, 1956, was chosen to illustrate low-altitude oscillatory temperature behavior which occurs in some areas.

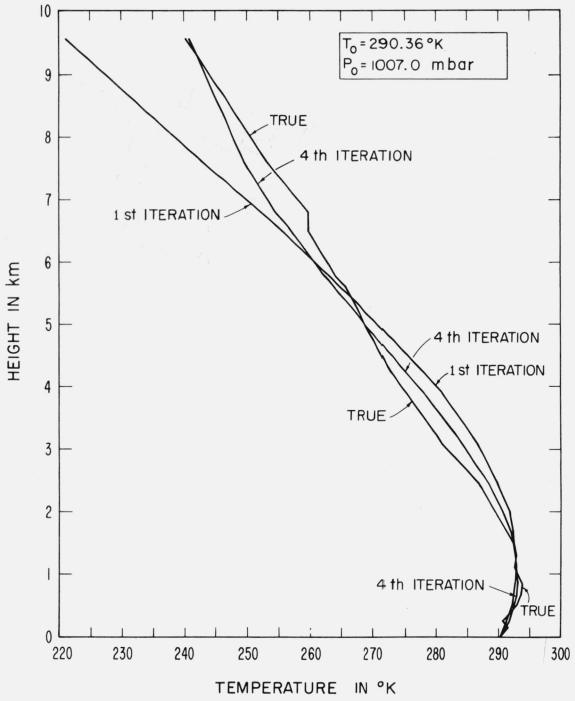

FIGURE 7. *Temperature profile determined by inversion of brightness temperature equation for Dakar, Senegal.*

For seven frequencies and a fifth-degree polynomial, an rms error of 2.2 °K and 0.507 mbar in temperature and pressure was obtained up to the 10.4-km level after four iterations.

It is also important to determine the effect of varying the degree of the polynomial on the error in T and on the rate of convergence. In table 2, the rms error in T and P are shown as a function of iteration number for a third, fourth, and fifth-degree polynomial.

TABLE 2. *The rms error in* T *and* P *up to* h = *10.4 km as a function of iteration number and polynomial degree for Dakar, Senegal, February 2, 1956.*

Iteration	3d-deg. poly.		4th-deg. poly.		5th-deg. poly.	
	rms error in T	rms error in P	rms error in T	rms error in P	rms error in T	rms error in P
	°K	*mbar*	°K	*mbar*	°K	*mbar*
1	5.5	3.1	6.5	2.3	6.6	2.2
2	6.0	3.6	4.2	1.6	2.5	0.4
3	6.1	3.6	4.2	1.7	2.2	0.6
4	6.0	3.6	4.2	1.7	2.2	0.5
5	6.0	3.6	4.2	1.7	2.2	0.5

The rates of convergence for this profile are not as spectacular as those of the Denver profile because a much more realistic first approximation for the absorption coefficients was used (an exponential model with statistically determined scale heights was the 0th approximation). It is easily seen that iteration does not improve the temperature solution for a low-degree polynomial (when there are not a sufficient number of adjustable parameters) over a best statistical estimate. For higher degree polynomials, a two- or three-to-one improvement can be obtained by iteration.

There is an upper limit, however, to the polynomial degree for a fixed number of frequencies which can be successfully used. This limit is imposed by the presence of errors both in the brightness temperature and in the first estimation of the absorption.

Finite errors will be present in any physical measurement of brightness temperature. Any such error in T_b will induce errors into the derived temperature profile. It is important therefore to have some estimate of the amount of measurement error in T_b which is tolerable for a physically meaningful temperature distribution. In the calculations reported here, two different types of errors were introduced, alternating and constant. The first type was introduced by adding $(-)^n|\delta T_b|$ to the nth T_b (the T_b's were arranged in ascending order). This set is referred to as type a. The set obtained by adding $(-)^{n+1}|\delta T_b|$ to the nth T_b is referred to as b. In figure 8 are shown the temperature distributions computed from the a and b sets of $|\delta T_b| = 1.25$ °K. The maximum error in the temperature distribution was about 10 °K for this magnitude of $|\delta T_b|$. The rms errors of a and b up to the 10.4-km level were 7.6 and 6.6 °K, respectively. Table 3 shows the results of various error calculations. It is to be noted that the iteration diverged for $|\delta T_b| = 2.5$ °K, case a, and that the effect of errors increased rapidly above $|\delta T_b| = 1.0$ °K. It is also important that no essential difference exists between the exact and 0.5° cases. This indicated that meaningful atmospheric information can be obtained from radiation measurements that possess a sufficiently small, but finite, error.

The effect of constant errors in T_b on the derived temperature profile is not as serious as "alternating" errors as discussed in the last paragraph. For an "alternating" error of magnitude 2 °K, the iteration sequence was near its radius of convergence; for a constant error of the same magnitude, the rms errors up to 10.4 km are only 6.1 and 4.3 °K for positive and negative errors, respectively. The derived profiles in the presence of these errors are plotted in figure 9. Similar errors of + and − 1 °K gave rms errors in temperature of 4.0 and 2.3 °K, respectively, up to 10.4 km. A much more meaningful analysis of the effect of errors in T_b on the derived temperature structure could be achieved by introducing in some suitable fashion random errors in the set of brightness temperatures. This was not attempted here because of excessive computer cost.

TABLE 3. *Results of error calculations*

Error in T_b	Case	S.E. (T) in °K up to 10.4 km
°K		
2.5	a	∞
	b	9.3
2.0	a	25.5
	b	8.6
1.5	a	12.8
	b	7.4
1.25	a	7.6
	b	6.6
1.0	a	4.9
	b	5.7
0.5	a	2.6
	b	3.8
0.0		2.2

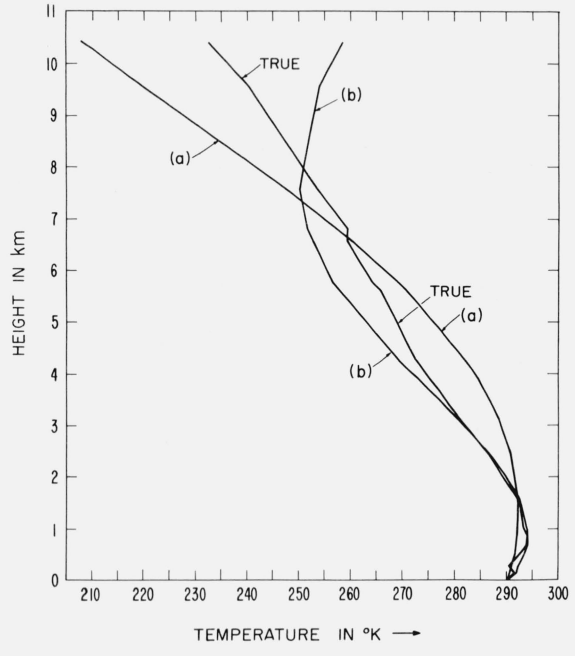

FIGURE 8. *Effect of alternating errors of magnitude 1.25 °K in brightness temperature on the reconstruction of the temperature profile.*

Case (a)—errors of $(-)^n|\delta T_b|$ added to the nth brightness temperature (arranged in ascending order). Case (b)—errors of $(-)^{n+1}|\delta T_b|$ added to the nth brightness temperature.

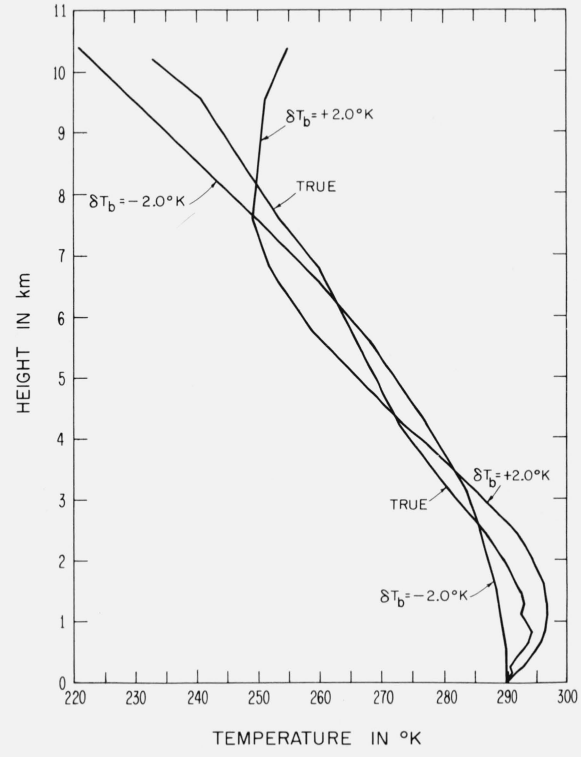

FIGURE 9. *Effect of constant magnitude errors in the brightness temperature on the reconstruction of the temperature profile.*

6. Conclusion

The mathematical method of inversion presented here appears capable, under certain restrictions, of recovering the thermal profile of the troposphere from a set of sufficiently accurate microwave (50 to 55 Gc/s) radiation measurements of a cloudless atmosphere. A tolerable amount of measurement error in the brightness temperature appears to be of order 0.5 °K.

The principle limitations (or approximations) of the technique appear to be the neglect of the water vapor emission (not valid under humid conditions) and the neglect of scattering (not valid when clouds are present in the main beam of a highly directional antenna). The contribution of water vapor could possibly be accounted for by simultaneous radiation measurements on the 22.2 Gc/s water vapor line. The uncertainties inherent in line width calculations can be at least partially removed by simultaneous measurements of the brightness temperature and the atmospheric profile above the radiometer.

7. Appendix A

The quantity of interest, $K(\nu,i)$, defined by (19), may be expressed as linear combination of functions of the form

$$M(n)=\int_0^H h^n\,\alpha(h)e^{-\int_0^h \alpha(h')dh'}\,dh. \tag{A1}$$

For notational convenience, the subscript ν has been omitted. We wish to evaluate (A1) under the assumption that the nonzero $\alpha(h)$ may be interpolated exponentially within any height interval:

$$\alpha(h)=\alpha(h_{i-1})e^{-\frac{h-h_{i-1}}{H_i}},\quad h_{i-1}\leq h\leq h_i, \tag{A2}$$

where

$$\frac{1}{H_i}\equiv-\frac{ln\,\dfrac{\alpha(h_i)}{\alpha(h_{i-1})}}{h_i-h_{i-1}},$$

$$h_0=0,$$

and

$$h_N=H.$$

We write

$$M(n)=\sum_{j=1}^{N}\int_{h_{j-1}}^{h_j} h^n\alpha(h)e^{-\int_0^h \alpha(h')dh'}dh$$

$$=\sum_{j=1}^{N} e^{-[\tau_{j-1}+\alpha(h_{j-1})H_j-h_{j-1}/H_j]}\,g(n,j), \tag{A3}$$

where

$$\tau_j=\sum_{i=1}^{j}\alpha(h_{i-1})H_i(1-e^{-\frac{h_i-h_{i-1}}{H_i}}),\ j=1,2,\ldots,N,$$

$$\tau_0=0$$

and

$$g(n,j)=\int_{h_{j-1}}^{h_j} h^n e^{-\frac{h}{H_j}}e^{\alpha(h_{j-1})H_j}e^{-\frac{h-h_{j-1}}{H_j}}dh,\ n=0,1,\ldots.$$

The functions $g(n, j)$ presumably can not be expressed in closed form. Instead, we express them as an infinite sum of integrals, each of which can be evaluated in closed form. This sum has been found to converge rapidly for $0\leq\alpha\leq 10$, $0\leq H\leq 20$. The integral defining $g(n, j)$ is of the form

$$I=\int_\alpha^\beta x^n e^{ax}e^{be^{-cx}}dx. \tag{A4}$$

By using a MacLaurin expansion for the second exponential term, we arrive at

$$I=\sum_{i=0}^{\infty}\frac{b^iA_{i,n}}{i!}, \tag{A5}$$

where

$$A_{i,n}=\int_\alpha^\beta x^n e^{(a-ci)x}dx.$$

The $A_{i,n}$ are easily obtainable from any standard table of integrals. The series defined by (A5) converges for any finite value of b or $A_{i,n}$ as may be seen by comparison with the series for e^{Ax}.

Thus, by making the correspondence $\alpha\rightarrow h_{j-1}$, $\beta\rightarrow h_j$, $a\rightarrow -1/H_j$, $b\rightarrow\alpha(h_{j-1})\,H_je^{h_{j-1}/H_j}$, and $c\rightarrow 1/H_j$, we have succeeded in evaluating (A1).

The author expresses his gratitude to R. L. Abbott and M. T. Decker for stimulating discussions and for continued encouragement during the performance of this work. The author also acknowledges A. E. Goertz for clarification of certain points concerning this line width.

8. References

Abbott, R. L. (1964), Width of the microwave lines of oxygen and their relationship to the thermal noise emission spectrum of the atmosphere, Proc. 3rd Symp. on Remote Sensing of the Environment, Univ. of Michigan, Ann Arbor, Michigan.

Artman, J. O. (1953), Absorption of microwaves by oxygen in the millimeter wavelength region, Columbia Radiation Laboratory Report, June, Columbia Univ., New York, N.Y.

Barrett, A. H., and V. K. Chung (1962), A method for the determination of high altitude water vapor abundance from ground-based microwave observations, J. Geophys. Res. **67**, No. 11, 4259–4266.

Becker, G. E., and S. H. Autler (1946), Water vapor absorption of electromagnetic radiation in the centimeter wave-length range, Phys. Rev. **70**, No. 5, 300–307.

Benedict, W. S., and L. D. Kaplan (1959), Calculations of line widths in H_2O-N_2, J. Chem. Phys. **30**, No. 2, 388–399.

Benedict, W. S., and L. D. Kaplan (1964), Calculations of line widths in H_2O-H_2O and H_2O-O_2 collisions, J. Quant. Spectr. Radiative Transfer **4**, No. 3, 453–469.

Chandrasekhar, S. (1960), Radiative Transfer, p. 1 (Dover Publications, New York, N.Y.).

Drake, F. D., and H. I. Ewen (1958), A broad-band microwave source comparison radiometer for advanced research in radio astronomy, Proc. IRE **46,** No. 1, 53–60.
Forward, R. L., and F. Rickey (1960), Effects of external noise on radar performance, Microwave J. **3,** No. 12, 73–80.
Fow, B. R. (1964), Atmospheric temperature structure from the microwave emission of oxygen, Masters Thesis, MIT.
Fryberger, D., and E. F. Uretz (1961), Some considerations concerning the measurement of the atmospheric temperature field by electromagnetic means, IRE Trans. Mil. Electron. **MIL-5,** No. 4, 279–285.
Goody, R. M. (1964), Atmospheric Radiation, p. 29 (Oxford, Clarendon Press).
Hewson, E. W., and R. W. Langley (1944), Meteorology, Theoretical and Applied, p. 19 (John Wiley & Sons, New York, N.Y.).
Meeks, M. L., and A. E. Lilley (1963), The microwave spectrum of oxygen in the earth's atmosphere, J. Geophys. Res. **68,** No. 6, 1683–1703.
Morse, P. M., and H. Feshback (1953), Methods of Theoretical Physics, Part 1, p. 925 (McGraw-Hill Book Co., Inc., New York, N.Y.).
Phillips, D. L. (1962), A technique for the numerical solution of certain integral equations of the first kind, J. Assoc. Computing Machinery **9,** 84–97.
Schiff, L. I. (1955), Quantum Mechanics, 2d ed., p. 261 (McGraw-Hill Book Co., Inc., New York, N.Y.).
Tinkham, M., and M. W. P. Strandberg (1955), Line breadths in the microwave emission spectrum of oxygen, Phys. Rev. **99,** No. 2, 537–539.
Tricomi, F. G. (1957), Integral Equations, p. 3 (Interscience Publ., Inc., New York, N.Y.).
Van Vleck, J. N. (1947a), The absorption of microwaves by oxygen, Phys. Rev. **71,** No. 7, 413–424.
Van Vleck, J. N. (1947b), The absorption of microwaves by uncondensed water vapor, Phys. Rev. **71,** No. 7, 425–433.
Zimmerer, R. W., and M. Mizushima (1961), Precise measurement of the microwave absorption frequencies of the oxygen molecule and the velocity of light, Phys. Rev. **121,** No. 1, 152–155.

(Paper 69D9–553)